Available online at www.sciencedirect.com
ScienceDirect
Earth and Planetary Science Letters 258 (2007) 378–396
EPSL
www.elsevier.com/locate/epsl

Micrometer scale carbon isotopic study of bitumen associated with Athabasca uranium deposits: Constraints on the genetic relationship with petroleum source-rocks and the abiogenic origin hypothesis

L. Sangély [a,b,*], M. Chaussidon [b], R. Michels [a], M. Brouand [a], M. Cuney [a], V. Huault [a], P. Landais [a,c]

[a] UMR 7566 G2R-CNRS, BP 239, Bd des Aiguillettes, 54506 Vandoeuvre-lès-Nancy Cedex, France
[b] CRPG-CNRS, BP 20, 15 rue Notre Dame des Pauvres, 54501 Vandoeuvre-lès-Nancy Cedex, France
[c] ANDRA, 1-7 rue Jean Monnet, 92298 Chatenay-Malabry Cedex, France

Received 30 June 2006; received in revised form 7 March 2007; accepted 7 March 2007
Available online 16 March 2007
Editor: R.W. Carlson

Abstract

In situ analytical techniques – Fourier transform infrared microspectroscopy (μFTIR) and ion microprobe – have been used to unravel the origin of solid bitumen associated with the uranium deposits of Athabasca (Saskatchewan, Canada). Both aliphaticity and carbon isotopic compositions within the samples are heterogeneous but spatially organized in concentric zonations at the micrometer scale. Finally, the $\delta^{13}C$ values are positively correlated to the aliphatic contents over an extremely large isotopic range from ~−49‰ to ~−31‰. We infer that this positive correlation may be related to the carbon isotopic fractionations associated with the synthesis of bitumen through the catalytic hydrogenation of CO_2, rather than the result of pre-existing petroleum product precipitation and/or alteration (such as radiolysis). This explanation is consistent with (i) published results of abiogenic synthesis experiments, in which the differences in $\delta^{13}C$ values between saturated and unsaturated hydrocarbons range from +2 and +19‰, in contrast to the differences systematically observed in conventional bitumen and petroleum ranging from 0‰ to −4‰; (ii) the absence of a similar positive correlation between aliphatic contents and $\delta^{13}C$ values in the other bitumen analyzed in the present study, for which a biogenic origin has been unequivocally established (samples from Oklo, Gabon, and Lodève, France, uranium deposits); (iii) the presence of CO_2 and H_2 in the gas-phase of fluid inclusions in the Athabasca uranium deposits, H_2 resulting from water radiolysis.

The present results suggest that the $\delta^{13}C$ vs. aliphaticity correlation could be used as a criterion to discriminate between abiogenic vs. biogenic origin of macromolecular organic matter.

Keywords: organic carbon isotopes; secondary ion mass spectrometry; bitumen; uranium deposits; Athabasca; abiogenic synthesis

1. Introduction

Most Mid-Proterozoic uranium deposits of the Athabasca Basin (northern Saskatchewan, Canada) contain

* Corresponding author. Present address: C.E.A., DIF/DASE/SRCE, BP 12, 91680 Bruyères-le-Châtel, France. Tel.: +33 1 6926 4214; fax: +33 1 6926 7065.
E-mail address: laure.sangely@cea.fr (L. Sangély).

0012-821X/$ - see front matter © 2007 Published by Elsevier B.V.
doi:10.1016/j.epsl.2007.03.018

small amounts of organic matter within an area restricted to ~50 m around the mineralized bodies. Organic matter is hosted in brecciated, hydrothermally altered rocks of the Archean to Paleoproterozoic metamorphosed basement and the Late Paleoproterozoic to Mesoproterozoic sedimentary cover [1–4]. This organic matter has been identified as solid bitumen (i.e. allochtonous organic matter found within rocks in the form of a non-disseminated solid phase). Bitumen is generally considered as deriving from i) the thermal maturation of kerogen in sedimentary rocks or ii) the alteration of petroleum (e.g. biodegradation, asphaltenes precipitation, thermal alteration, oxido-reduction reactions) [5]. Since the discovery of the uranium deposits of the Athabasca in the late 60's, the origin of the associated bitumen has remained an unresolved issue despite numerous petrographic and geochemical studies [1–4]. Organic geochemistry studies demonstrate the potential for petroleum generation of several regional rock units ranging from Paleoproterozoic to Paleozoic in age. However, there is no consensus on which source-rock is actually related to the bitumen associated with uranium deposits.

Protoliths to the metasedimentary rocks of the basement have been identified as Paleoproterozoic organic-rich pelites, psammites, and minor carbonates deposited in a continental margin environmental setting. The Mesoproterozoic sedimentary rocks includes fluvial to shallow marine quartz-rich sandstone deposited in a near-shore, shallow shelf environment as well as marine discontinuous beds of siltstones, mudstones, shales, and stromatolitic carbonates [6]. Occurrences of bitumen are widely reported in uranium deposits hosted in such fluvio-deltaic sediments from continental or marginal

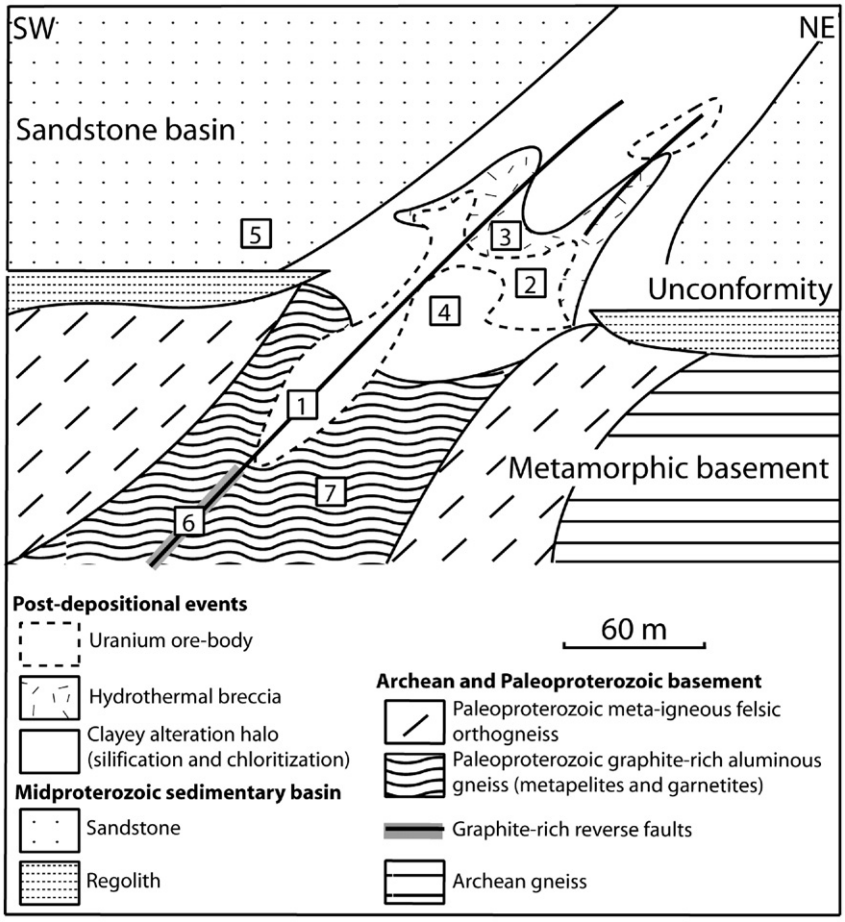

Fig. 1. Schematic cross-section of the study area in Athabasca, modified after [18] displaying the occurrences of solid bitumen and graphite within the unconformity-related uranium deposit (Shea Creek exploration zone, Northern Saskatchewan, Canada). Numbers refer to bitumen occurrences located: in the uranium-mineralization in the basement (1) and the sedimentary cover (2), in the breccia body (3), in the clayey alteration haloes (4), in the sandstone cover (5). Numbers (6) and (7) correspond to graphite occurrences within the basement: in reverse faults and in metasedimentary rocks (here a meta-greywacke), respectively.

marine plain environments. However, depositional and formational setting commonly accepted stands in contrast to some features of the Athabasca.

For instance, genetic link between petroleum source-rocks and bitumen associated with the Paleoproterozoic uranium deposits of Oklo (Gabon) could be established on the basis of obvious geometric relationships [7]. Bitumen-hosting deltaic sandstones are spatially associated with marine black shales in structures similar to fault trap petroleum systems. The observation of mineralization paragenesis led some authors to propose that oils may have acted as a reductant to precipitate uraninite from U-bearing hydrothermal solutions permeating into oil reservoirs [8]. As a result, the liquid hydrocarbons may have been simultaneously oxidized into solid bitumen. Similar formational process has been proposed for the bitumen associated with the uranium deposits of Lodève (France). In addition, the genetic link between bitumen hosted in the reservoir facies (Cambrian karstified basement, Permian fluvial conglomerates, deltaic sandstones and siltstones interbedded with pyroclastic horizons) and the adjacent Permian lacustrine petroleum source-rocks has been confirmed by geochemical study [9]. Sterane and terpane biomarker fingerprints in reservoir facies and source-rocks has been shown to be consistent (Landais and Connan, 1986).

Uranium deposits of the Athabasca differ from the above-cited localities by the paragenesis sequence of mineralization. It is commonly accepted that bitumen post-date uranium minerals corresponding to the main mineralization stage, suggesting that oils may have played no role in uranium precipitation [4]. This is consistent with a recent study that points out the lack of hydrocarbons in the gas-phase of pre- and syn-mineralization fluid inclusions in quartz overgrowth [10]. It has been proposed that bitumen could rather have precipitated in the environment of the uranium deposits through radiolytic polymerization of oil on contact of uranium-bearing minerals. In addition, spatial relationship between potential source-rocks in the Athabasca Basin and the bitumen-hosting rocks in the vicinity of uranium deposits does not display obvious petroleum system-like architectural features [1]. Known potential petroleum source-rocks in the Athabasca Basin includes i) the Phanerozoic black shales responsible for the generation of the bitumen regionally distributed in the Early Cretaceous Athabasca tar sands (i.e. Late Devonian–Early Missippian Exshaw Formation) ii) the Mesoproterozoic siltstones and mudstones of the Douglas Formation and dolostones of the Carlswell Formation. The stratigraphic localization of these potential petroleum source-rocks in the Athabasca Basin implies that the oil generated from these formations may have migrated downward through the 1500 m thick sandstones of the Athabasca Group to reach the unconformity and the brecciated basement. The bitumen is actually distributed as uranium mineralization along structures consisting in graphite-rich shear faults rooted in the Paleoproterozoic metamorphosed basement. It should be noted that molecular studies by gas chromatography-mass spectrometry (GC-MS) appeared of little help in characterizing the origin the bitumen associated with the uranium deposits of the Athabasca. As thermally or radiolytically altered organic matter, Precambrian uraniferous bitumen generally

Fig. 2. Photographs illustrating occurrences of bitumen and graphite within the different host-rocks (see arrows) and the corresponding microscopic textures (numbers correspond to occurrences shown in Fig. 1). 1-a: Bitumen nodules observed in fractures within uranium mineralized bodies in the basement (Q = quartz, P = pyrite, D = dravite). 1-b: Back-scattered electron SEM micrograph of a section in a corresponding bitumen nodule. The fibrous aspect of bitumen nodules is due to radial internal structures. The concentric zoning (darker rims underlined by dashed curves) results from a depletion in uranium at the periphery of nodules relative to the core. 2-a: Massive layered bitumen and 2-b: bitumen nodules (SEM micrograph of a nodule separated from its host-rock), both observed within the uranium-ores of the sandstone cover. 2-c: SEM micrograph of a corresponding bitumen nodule in section. The lighter rim is enriched in uranium and sulfur relative to the core and corresponds to the light areas observed at the surface of nodules in 2-b. 3-a: bitumen within the breccia body. SEM micrograph of corresponding bitumen nodules, 3-b: bitumen nodule separated from its clayey host-rock, 3-c: bitumen nodule in section. The progressive concentric zoning (lighter rims underlined by dashed curves) results from an enrichment in sulfur, chlorine and calcium. Pyrite micro-inclusions (white grains) display a parallel corona distribution mostly limited to the core of the nodules. Bitumen samples in panels 3-a, -b, and -c correspond to the same occurrence as the nodules analyzed in Fig. 6. 4-a: Layered bitumen and 4-b: bitumen patches, both observed within the alteration haloes in sandstone. 4-c: SEM micrograph of a bitumen patch in section. Large minerals enclosed in bitumen are quartz (dark grey), pyrite (light grey) and galena (white), micro-inclusions are uraninite. 5-a: bitumen occurring in quartz cavities within the sandstone cover. 5-b: Secondary electron SEM micrograph of quartz cavities showing the bitumen nodules associated with pyrite cubes. 5-c: Back scattered electron SEM micrograph of a corresponding bitumen nodule in section. The radial internal structures resemble those observed in bitumen nodules within the basement (1-b). The concentric zoning (lighter rim underlined by dashed curve) is due to an enrichment in uranium at the periphery of the nodule. 6-a: massive graphite associated with sulfide in fracture within the shear zone affecting basement aluminous gneiss. 6-b: Secondary electron SEM micrograph of the corresponding material showing well-crystallized graphite flakes. 7: Reflected light photograph revealing the occurrence of graphite distributed along the foliation of meta-sedimentary rocks of the basement. Graphite occurs together with quartz, muscovite, chlorite and anatase. The identification of graphite in basement rocks is also supported by Raman microspectroscopy. [19] reported first-order Raman spectra exhibiting a single band located around 1575 cm^{-1} which corresponds to C–C vibrations in aromatic layers.

contains (i) only trace amounts of molecules extractible by common organic solvents and (ii) no detectable level of biomarker compounds are released from this bitumen during on-line pyrolysis [9].

Carbon isotopic study may provide some information about bitumen origin. $\delta^{13}C$ value of bitumen depends on both i) $\delta^{13}C$ value of kerogen in the related source-rock and ii) the physical and chemical processes involved in bitumen formation and alteration. Bulk-rock analyses reported in a previous study revealed a noteworthy contrast in $\delta^{13}C$ value between two spatially independent bitumen occurrences [11] (~−28‰ and ~−49‰ at Cigar Lake and Cluff Lake, respectively). It is still unclear whether the isotopic variability observed between the two localities results from the contribution of several source-rocks with different $\delta^{13}C$ values or from different bitumen

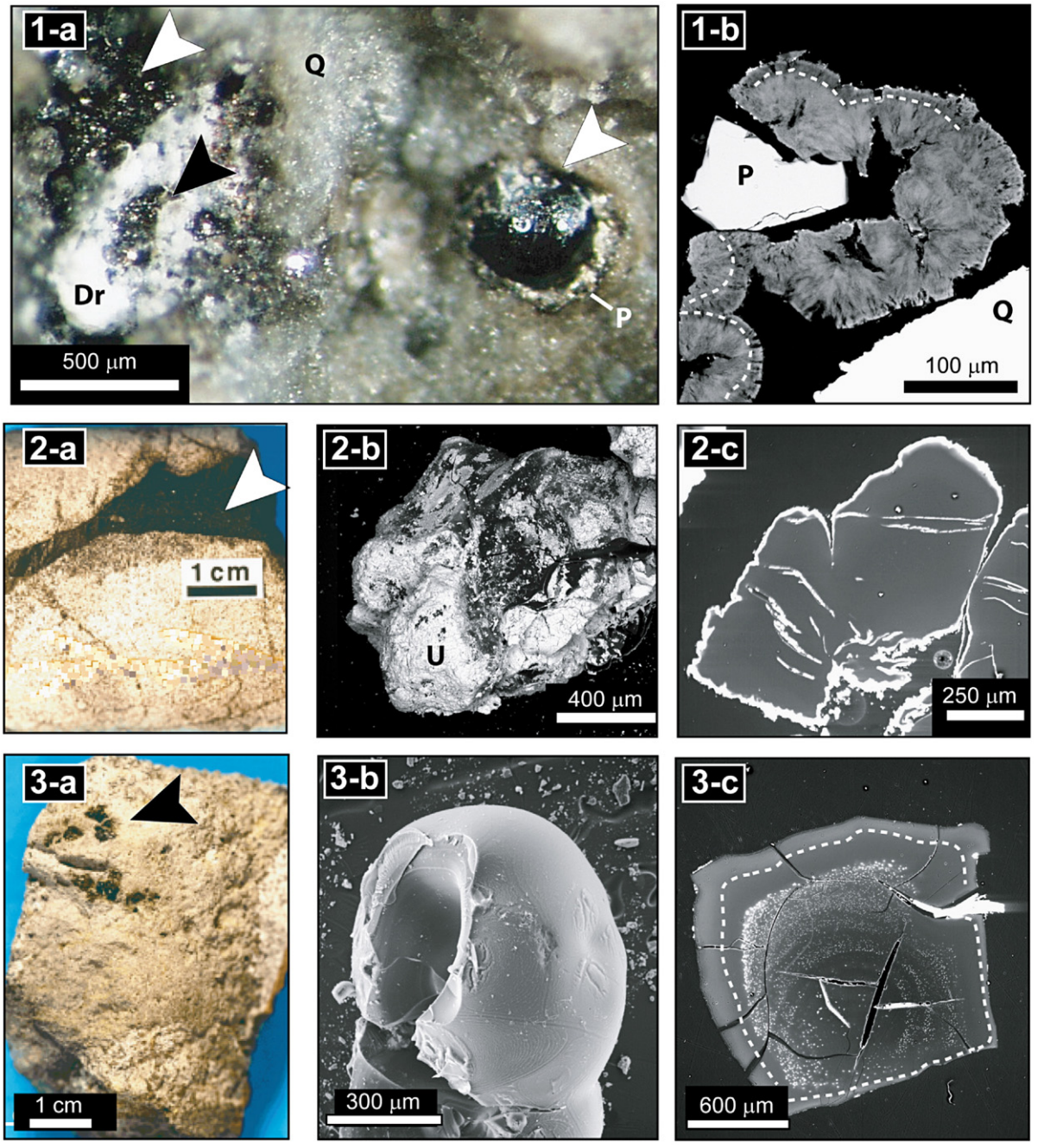

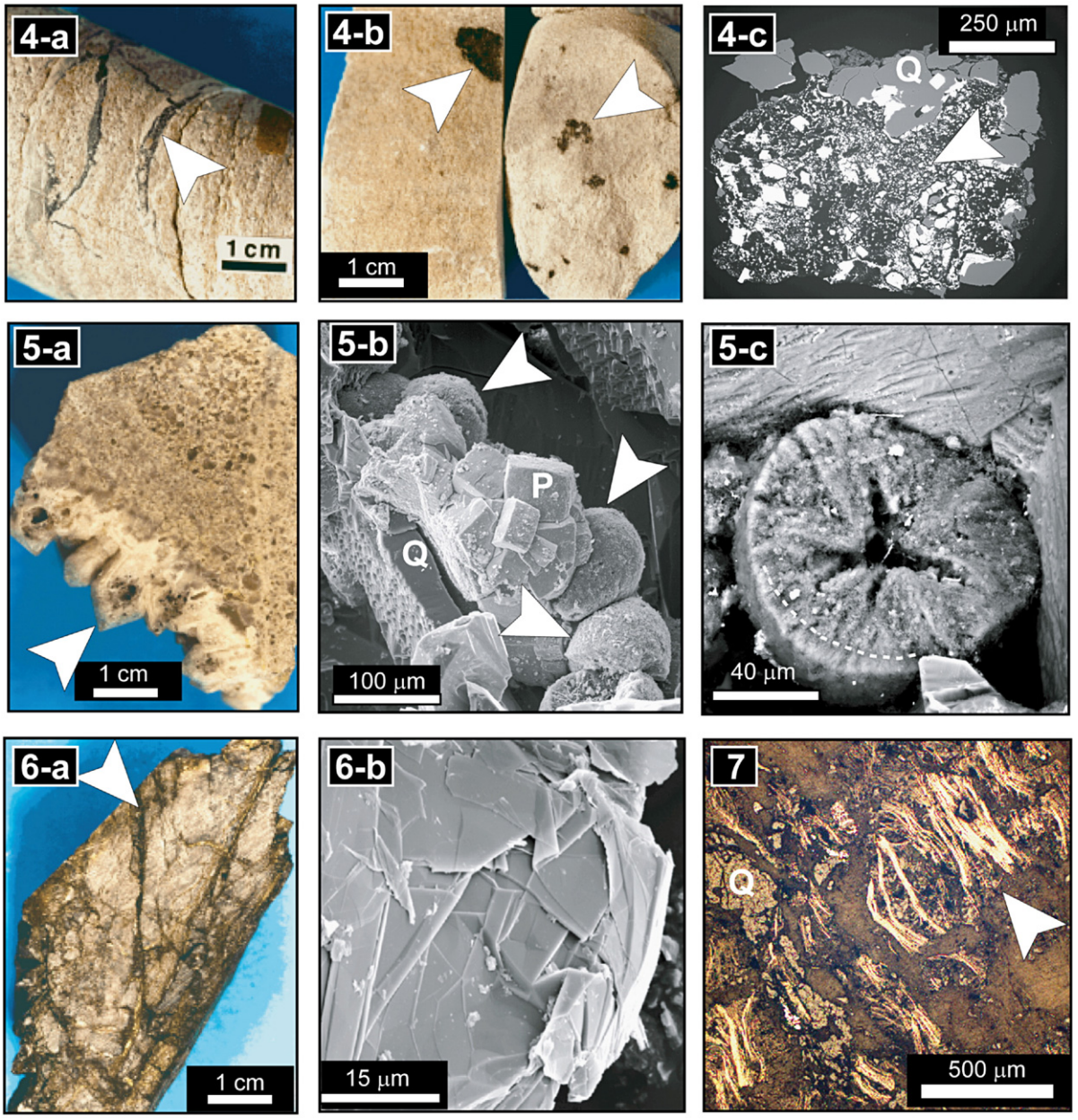

Fig. 2 (*continued*).

formation/alteration histories. Addressing this issue in the particular context of uranium deposits requires to evaluate the influence of radiation-induced alteration (i.e. radiolysis) on $\delta^{13}C$ values of bitumen. The passage of particles through bitumen may significantly alter the chemical properties of irradiated medium through C-chain scission and crosslinking reactions. Bitumen C-chain scission reactions resulting in the production of hydrocarbon has been shown to fractionate C-isotopes [12]. The classical way to evaluate the influence of radiolysis is to investigate the relationships between $\delta^{13}C$ values, uranium content and/or some relevant chemical properties in the bitumen, e.g. [12,13]. However, difficulties arise in the interpretation of such bulk rock analytical data because radiolysis is a spatially localized process. The radiation dose absorbed by the bitumen is applicable only to the mass of the material reached by the particles emitted from uranium-bearing minerals. Most of uranium energy decay is

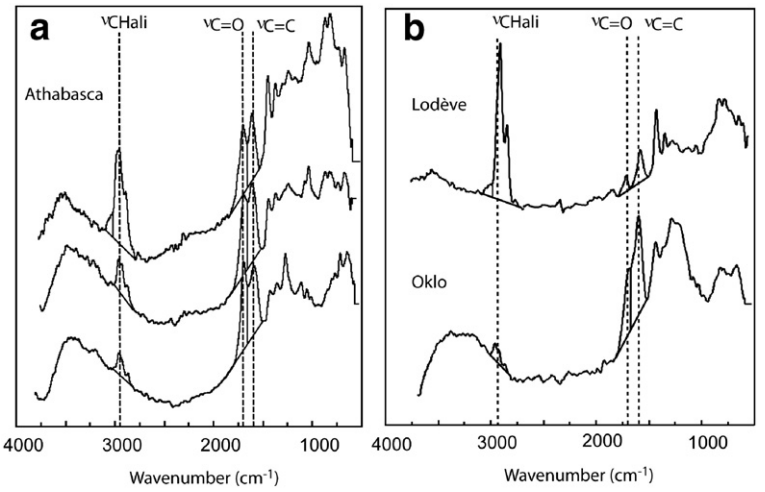

Fig. 3. Absorption index spectra obtained using specular reflection Fourier transform infrared microspectroscopy on bitumen samples from the Athabasca (A), the Oklo and Lodève (B) uranium deposits. Numbers refer to band assignments, 1: ν_{CHali}=3000–2800 cm^{-1}, 2: $\nu_{C=O}$=1800–1655 cm^{-1}, $\nu_{C=Caro}$=1655–1520 cm^{-1}. Solid lines depict an example of peak fitting according the so-called "valley-to-valley method".

released in the form of α particles. The range of α particles in organic matter (i.e. the distance of penetration up from which the energy of the particle drops below the point that the particles no longer alter the material) has been estimated to 50 μm. This is supported by microscopy studies commonly reporting increases in reflectance and anisotropy of bitumen <50 μm from uranium minerals [2]. These changes have been interpreted as resulting from the development of aromatic structures displaying a short range ordering.

The aim of this work was to investigate in situ the variability in δ^{13}C values and chemical composition of the bitumen associated with the uranium deposits of the Athabasca in order to get some clues on their origin. In the present study, we developed a precise in situ approach combining Fourier transform infrared microspectroscopy (μFTIR) in specular reflection mode [14] and multicollector ion microprobe sensing to investigate δ^{13}C variations as a function of chemical composition at the micrometer scale in solid bitumen samples [15]. A set of 9 standards representative of the chemical variability of organic matter was prepared to precisely calibrate matrix effects during ion microprobe analysis. External precision of the analyses was ±0.7‰ (1σ) on the δ^{13}C values. Because no information is available in the literature on δ^{13}C variability intrinsic to "conventional" bitumen at the micrometer scale, we also studied two other bitumen samples from the spatially independent uranium deposits of Oklo (Paleoproterozoic, Gabon) and Lodève (Permian, SE France). Both additional samples have been selected because their origin and their formation processes are well understood [7,9].

2. Geological setting

2.1. Athabasca

The Athabasca uranium ore-bodies are spatially associated with graphite-bearing faults in the vicinity of an unconformity between an Archean to Lower Proterozoic gneissic basement and a Mid-Proterozoic, non-metamorphosed sandstone basin [6,16] (Fig. 1). The major uranium mineralization stage has been dated at 1461±47 Ma [17]. Bitumen is found associated with the uranium mineralization from centimeter to decameter scale, in both the sandstone cover and the basement [1–4,11] (Fig. 1). Bitumen occurs in diverse host-rocks including brecciated gneiss, sandstone, sandstone-hosted breccias as well as clays within the alteration haloes of the mineralized bodies (Fig. 2). Bitumen can form more or less massive layers within fractures, patches as well as brittle millimeter size nodules. When present, bitumen displays total organic carbon contents in rocks ranging from 0.06 wt.% to 25 wt.% [2]. Reflectance and paragenesis data indicate that bitumen associated with U-deposits probably have formed during the hydrothermal event which took place between 1450 and 900 Ma at P–T conditions of 180±20 °C and 0.6 kbars [10]. Textural relations between uranium minerals and solid bitumen suggest that bitumen postdated mineralization [4].

2.2. Oklo

The Oklo uranium deposit is located in the Francevillian series (Paleoproterozoic) of the Franceville basin in Gabon. It is situated at the top of the basal formation overlaid by the black shales. The basal formation is mainly composed of conglomerates and fine to coarse grained sandstone deposited in a fluvial and deltaic environment. First oil migration event likely occurred ca. 2000 Ma ago, when black shales kerogen reached maximal burial temperature (~180 °C as estimated by fluid inclusion study [20]). Uranium bodies occur in tectonic structures affecting the Francevillian series, which correspond to the main characteristics of petroleum fault traps [7]. Bitumen occurs either associated with uranium in sandstone-conglomerate reservoirs overlain by impermeable black shales or in the sandstones and dolomites interbedded in the black shales. The overlying black shales have been shown to act as petroleum source-rocks for the bitumen

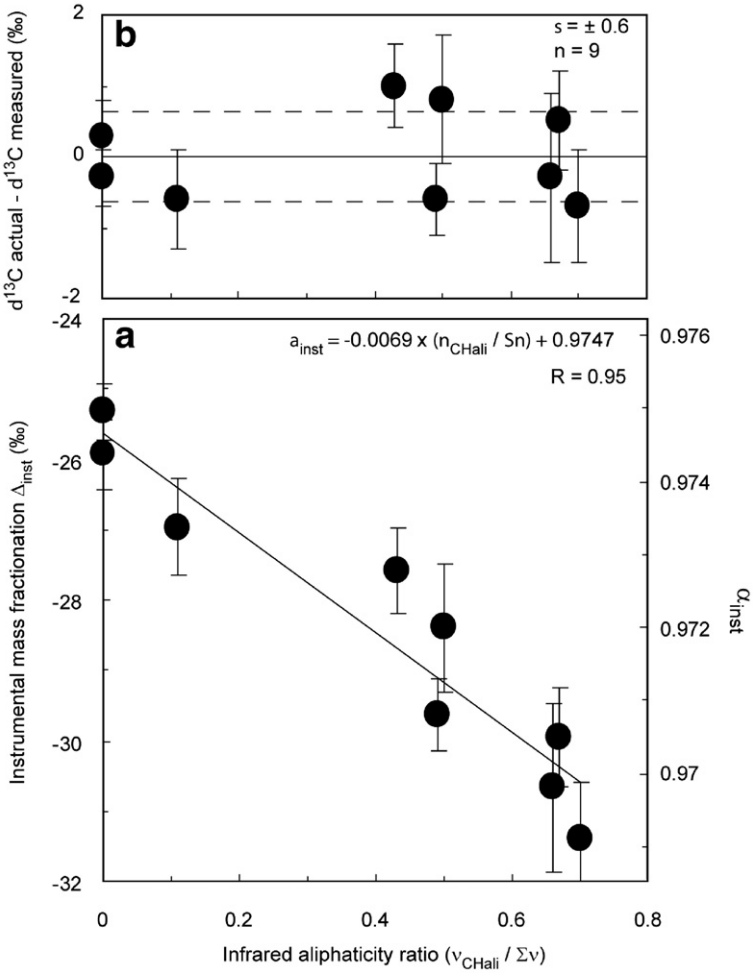

Fig. 4. Effects of the aliphaticity on instrumental mass fractionation (α_{inst}) during $\delta^{13}C$ measurements in organic matter for a set of 9 standards. In A: α_{inst} varied by ~0.005 (i.e. Δ_{inst} varied by ~5‰) over the set of standards and appeared negatively correlated to infrared aliphaticity ratios ($\nu_{CHali}/\Sigma\nu$), over a range from 0 (for graphite) to 0.7 (for alginite coal). Error bars on α_{inst} values correspond to the standard deviation over repeated analyses on each standard. The diameter of data points corresponds to the maximal absolute standard deviation in $\nu_{CHali}/\Sigma\nu$ obtained by repeated measurements on reference materials (i.e. ±0.02). In B: difference between ion microprobe $\delta^{13}C$ measurements corrected for instrumental mass fractionation and $\delta^{13}C$ values determined by conventional analysis as a function of infrared aliphaticity ratios in standard materials. The linear regression of measured α_{inst} values against aliphaticity ratios ($\alpha_{inst} = -0.0069 \times (\nu_{CHali}/\Sigma\nu) + 0.9747$, $R = 95$ — see panel A) has been used to calculate accurate α_{inst} values from aliphaticity ratios ($\nu_{CHali}/\Sigma\nu$) for each standard. Then, corrected ion microprobe $\delta^{13}C$ measurements have been calculated according to the relationship: $\delta^{13}C_{corr} = 1000 \times [(\delta^{13}C_{uncorr}/1000 + 1)/\alpha_{inst} - 1]$. The uncertainty due to the correction for instrumental mass fractionation has been evaluated to ~±0.2‰ ($\sigma/n^{1/2}$).

trapped in sandstones-conglomerates. Bitumen accounts for organic carbon contents ranging between 0.5 and 1 wt.%, continuously distributed throughout the sandstone-conglomerates of the Francevillian Series. Thermal alteration and interaction with oxidizing uranium-bearing fluids have been shown to be responsible for bitumen precipitation.

2.3. Lodève

The Lodève basin is located on the southern limit of the French Massif Central (France). Major mineralizations are located in the Autunian series (Permian) which include black shales and repeated sedimentary sequences of silty and dolomite facies in addition to some cineritic layers. Uranium mineralization is found mostly in association with bitumen occurring in reservoir facies (such as siltstones, cinerites as well as in fault breccias) which acted as migration pathways for the oils generated from the black shales of the Permian series. Two mineralization events have been dated at 173±6 and 108±5 Ma [21]. The genetic link between the bitumen and the petroleum source-rocks has been demonstrated by biomarkers studies [9]. Oil biodegradation and interaction with oxidizing uranium-bearing fluids have been shown to be responsible for bitumen precipitation [9].

3. Methods

3.1. Fourier transform infrared micro-spectroscopy

Fourier Transform microspectroscopy (μFTIR) spectra were acquired in specular reflection mode at a spatial resolution of 60 μm, according to a method described in [14]. Distinct absorption index bands due to stretching (ν), bending (δ), and out-of-plane deformation (γ) mode vibrations were observed (Fig. 3). Assignments of the infrared bands were determined after the tables available in [22,23]. Only bands related to stretching vibration mode were considered because they provided the most reproducible peak fitting results. The bands corresponding to wave numbers of 3000–2800 cm^{-1}, 1800–1655 cm^{-1}, and 1655–1520 cm^{-1} were related to aliphatic C–H (ν_{CHali}), carbonyl C═O ($\nu_{C=O}$), and aromatic C═C ($\nu_{C=Caro}$) bonds, respectively. Spectra in the ν_{CHali} range exhibit several (up to 4) more or less defined peaks corresponding to asymmetric and symmetric stretching vibrations in both –CH3 and –CH2-groups [24]. OMIC software was used to fit the bands of interest using the common method described in [23]. The baseline chosen for band intensity measurements was the "valley-to-valley" line. The precise determination of integration range for the different peaks depends on band profiles.

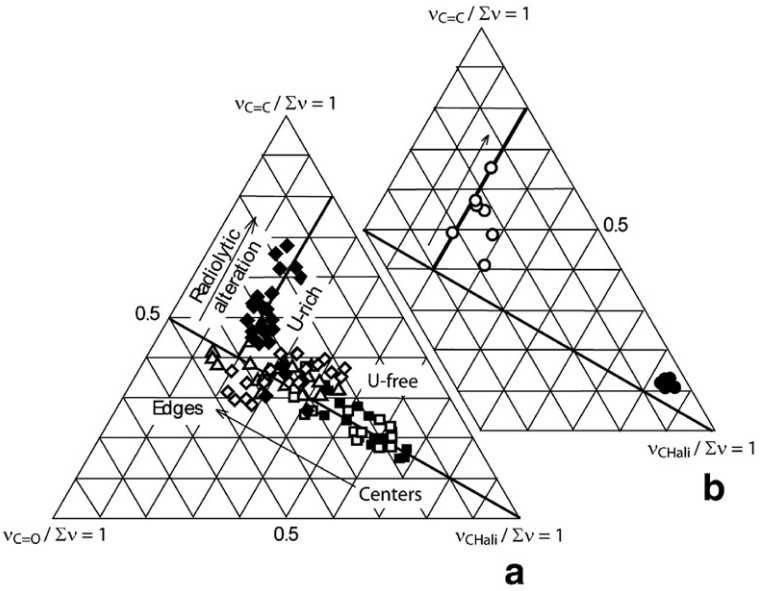

Fig. 5. Ternary plot showing the in situ relative intensities of stretching mode vibrations calculated for uranium deposits bitumen from μFTIR spectra. Relative intensities ν_{CHali},$\nu_{C=Caro}$, and $\nu_{C=O}$ correspond to aliphatic C–H, aromatic C═C, and C═O bonds, respectively. In a: Athabasca bitumen. Each symbol corresponds to a different nodule collected: within the ore-body (U=111 ppm, closed diamonds and open triangles), 25 m from the ore-body (U=14 ppm, open diamonds), about 1 m from the ore-body (U=4 ppm, open and closed squares). In b, bitumen from the Oklo (open circles) and Lodève (closed circles) uranium deposits.

In the case of well-defined peaks, integration limits correspond to the intersections between the peak and the baseline. In the case of peak overlapping, integration limits correspond to peak shoulders. An example of peak fitting is depicted in Fig. 3. Peak areas were used to calculate an aliphaticity ratio) which equals to $\nu_{CHali}/(\nu_{CHali}+\nu_{C=Caro}+\nu_{C=O})$. The reproducibility on $\nu_{CHali}/\Sigma\nu$ has been determined by repeated measurements ($n=4$) on several organic standards including resinite, vitrinite, and anthracite. The relative standard deviations over the 4 measurements range from 2% in aliphatic-rich materials ($\nu_{CHali}/\Sigma\nu \sim 0.7$) to 20% in aliphatic-poor materials ($\nu_{CHali}/\Sigma\nu \sim 0.1$). The uncertainty associated to $\nu_{CHali}/\Sigma\nu$ values given in the present dataset

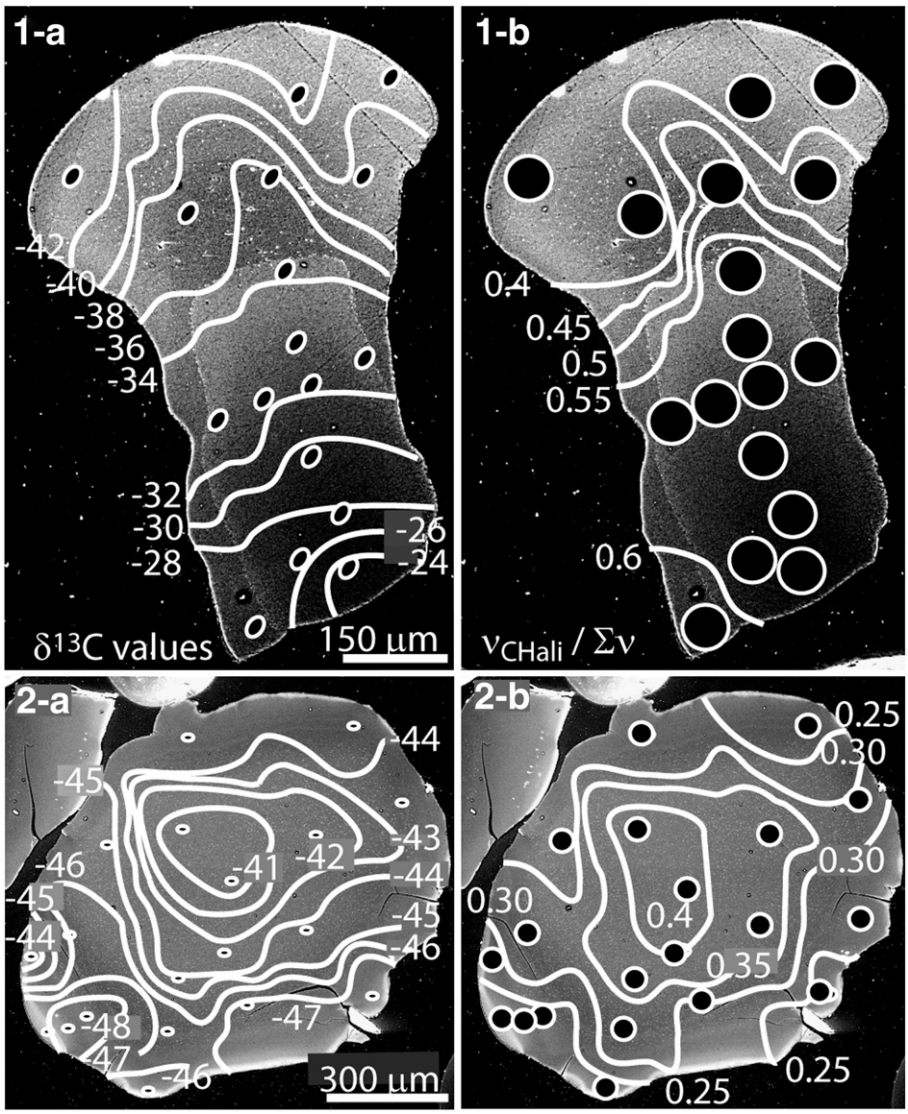

Fig. 6. Zonations in $\delta^{13}C$ values and in aliphaticity ratios observed within two bitumen nodules from Athabasca deposits. Both bitumen nodules come from the clayey breccias surrounding the mineralization (corresponding to occurrence number 3 on Fig. 1). Bitumen nodule in panels 1a–1b and 2a–2b corresponds to open squares and open diamonds on Fig. 5 and 7, respectively. Curves correspond to equal $\delta^{13}C$ (1a–2a) and $\nu_{CHali}/\Sigma\nu$ values (infrared aliphaticity ratio, 1b–2b). Black dots in panels 1a–2a and 1b–2b are ion microprobe holes and FTIR analysis areas, respectively. Gnuplot plotting program was used for data mapping. A grid (i.e. one data point at each mesh intersection) were created from the scattered data set (x, y, z), where x, y are the coordinates of analysed areas and z the corresponding measured values (i.e. $\delta^{13}C$ or $\nu CH_{ali}/\Sigma\nu$). The z values are computed as weighted averages of all scattered points' z values. Each data point is weighted inversely by its distance to from the grid point raised to the norm power (in this study the norm parameter was set to 4). Then, contour lines were generated by interpolating grid points. The use of grid-data mapping routine explains why the contour lines displayed in Fig. 6 differ from what would be obtained by direct interpolation between nearby data points. Spot dimensions are not taken into account in such mapping procedure since each measured value is attributed to a point (namely the center of analysis areas).

corresponds to the maximal absolute standard deviation obtained on standards (i.e. ±0.02).

3.2. Ion microprobe $\delta^{13}C$ measurements

The ion microprobe carbon isotope compositions reported hereafter were determined using the CAMECA IMS 1270 at CRPG-CNRS, Nancy, France. Analytical techniques developed for the present study are given elsewhere [15]. Carbon isotopic compositions are expressed in the conventional per mil delta notation relative to the Pee Dee Belemnite (PDB) marine carbonate standard ($\delta^{13}C$):

$$\delta^{13}C_{\text{sample}} = \left\{ \frac{^{13}C/^{12}C_{sample}}{^{13}C/^{12}C_{\text{PDB}}} - 1 \right\} \times 1000$$

where $^{13}C/^{12}C_{\text{PDB}} = 1.1237 \times 10^{-2}$.

Samples were mounted in epoxy resin. Polished sections were sputtered with primary beam of Cs^+ ions of 3–5 nA intensity accelerated to 20 keV impact energy. The primary ion beam was defocused using Kohler illumination to produce a roughly circular, flat-bottomed crater of ~20 μm diameter and ~1–2 μm depth. A normal-incidence electron flood gun was used to compensate for sample charging during analysis. Secondary negative carbon ions were accelerated at 10 keV without energy filtering, and analyzed at a mass resolution of ~5000 to resolve the interference between $^{12}CH^-$ and $^{13}C^-$. The $^{12}C^-$ and $^{13}C^-$ ions were counted in multi-collection mode on two Faraday cups. A within-run precision ~0.1‰ at 1σ standard error of the mean is typically achieved after ~2 min counting with a ^{12}C intensity of $\sim 5 \times 10^8$ cps. Approximately 20 measurements were performed on each sample, which resulted in a ~100–200 μm step grid. The major difficulty for this type of isotopic measurement is the calibration of the instrumental mass fractionation which can be very sensitive to matrix effects. For carbon, it is defined by:

$$\alpha_{\text{inst}} = \frac{(^{13}C/^{12}C)_{\text{measured}}}{(^{13}C/^{12}C)_{\text{true}}}$$

In addition, it can be reported in units of permil, calculated by the relationship:

$$\Delta_{\text{inst}} = 1000 \times \ln(\alpha_{\text{inst}})$$

Chemical and carbon isotopic compositions of standards (including graphites, anthracite, two vitrinite coals, two alginite coals, resinite coal, and type II kerogen) span a range from 0.04 to 1.75 in H/C atomic ratios and from −31.1‰ to −6.8‰ in $\delta^{13}C$ values. The reproducibility of repeated $\delta^{13}C$ measurements on standards ($n \sim 20$) (i.e. external precision) is ~±0.7‰ (1σ). It was observed that α_{inst} varies as a linear function of the aliphaticity in standards investigated, with typical values of 0.975 and 0.970 for aliphaticity ratios ($\nu_{\text{CHali}}/\Sigma\nu$) of 0 (graphite) and 0.7 (alginite coal), respectively (Fig. 4). The aliphaticity ratios of area previously analyzed for $\delta^{13}C$ were determined by μFTIR. We checked on standard materials that aliphaticity ratios measured by μFTIR were not affected by primary ion exposure [25]. The sampling depth of μFTIR (in the μm range) is much larger than the 10 nm depth chemically altered as the result of primary ion implantation and of differential sputtering rates during ion microprobe measurements. However, a slight polishing step was necessary to remove gold coating and to restore smooth and planar surface suitable for μFTIR used in reflection mode, when non-destructive μFTIR was not performed before ion microprobe analysis. The precision of the correction for matrix effects on α_{inst} is of ±0.2‰ (1σ standard error of the mean) over the whole range of aliphaticity. The precision of ion microprobe $\delta^{13}C$ measurements is estimated to be ~±0.7‰ (1σ) from the quadratic sum of the uncertainties derived from counting statistics (±0.1‰), the point-to-point reproducibility on standards

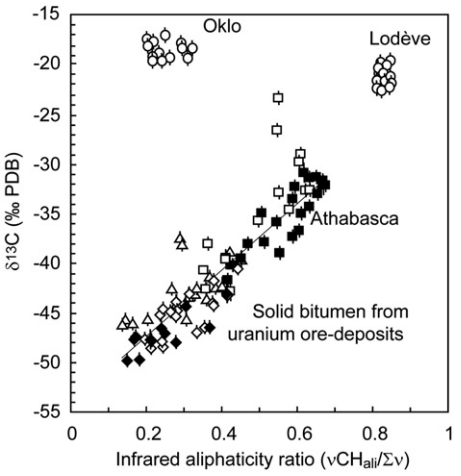

Fig. 7. Plot of $\delta^{13}C$ values against infrared aliphaticity ($\nu_{\text{CHali}}/\Sigma\nu$) for various bitumen from the Athabasca uranium deposits (all symbols but circles, each symbol corresponding to a different nodule) and bitumen from the Oklo and the Lodève uranium deposits (open circles). Error bars on ion microprobe $\delta^{13}C$ values are ±0.7‰. The diameter of data points corresponds to the maximal absolute standard deviation in $\nu_{\text{CHali}}/\Sigma\nu$ obtained by repeated measurements on reference materials (i.e. ±0.02).

(±0.6‰) and the correction for matrix effects on instrumental mass fractionation (±0.2‰).

4. Samples

4.1. Athabasca

The bitumen samples of Athabasca analyzed in the present study were collected from the Shea Creek uranium prospect, located 10 to 20 km south of the Carswell impact structure in the western part of the Athabasca basin (northern Saskatchewan, Canada). They were sampled from drill cores corresponding to an average depth of about 750 m. Rock samples enclosing non-fibrous bitumen nodules were collected in the ore-body occurring within the sandstone cover (corresponding to number 2 in Fig. 1, and numbers 2-b and 2-c in Fig. 2) as well as in clayey breccias surrounding the mineralization (corresponding to number 3 in Fig. 1, and numbers 3-b and 3-c in Fig. 2). Typical organic carbon content of the rock samples is less than 0.5 wt.%. The uranium content of the whole rock ranges between 100 ppm in barren samples and 10 wt.% in mineralized samples. The uranium content of the bitumen itself, after being mechanically isolated from the host-rock, ranges from 5 to 110 ppm. The H/C and O/C atomic ratios of the bitumen range between 0.6 and 0.7, and between 0.03 and 0.15, respectively [15].

4.2. Oklo

The Oklo bitumen sample comes from the uranium mine of Oklo, located 50 km northeast of Franceville in the northwestern edge of the Franceville basin (Gabon). It was collected from underground mining operation in a massive bitumen layer at a depth of about 300 m, near the core of the "natural fission reactor 10". This bitumen is strongly mineralized and encloses quartz relics remaining from the host sandstone. Its uranium and organic carbon content are 42 wt.% and 8.7 wt.%, respectively. Bitumen H/C and O/C ratios are 0.46 and 0.13, respectively [15].

4.3. Lodève

The Lodève bitumen sample was collected at the Mas Lavayre uranium mine, located 5 km southeast of Lodève, in the northwestern edge of the Lodève basin (SE, France). The sample was located in a massive, black and brittle bitumen layer hosted in siltstone from underground mining operation at a depth of about 300 m. Its uranium and organic carbon content are of 110 ppm and 86.1 wt.%, respectively. The bitumen H/C and O/C atomic ratio are 1.23 and 0.02, respectively [15].

5. Results

5.1. Fourier transform infrared micro-spectroscopy

Fourier transform infrared micro-spectroscopy spectra reveal that the relative aliphatic content is heterogeneous at the micrometer scale, within individual samples of bitumen of Athabasca. At the same scale, it is more homogeneous in the two other deposits (Figs. 3 and 5). In the Athabasca uranium deposits, ν_{CHali} decreases at a given $\nu_{C=Caro}/\nu_{C=O}$ and at the micrometer scale from centers to edges of each analyzed bitumen nodule. In addition, the ranges in aliphatic content vary between the different samples analyzed. No clear relationship appears between FTIR aliphaticity, uranium content of bitumen, and distance of samples to the mineralized bodies (see caption of Fig. 5). On the other hand, $\nu_{C=Caro}$ increases relative to $\nu_{C=O}$ at low ν_{CHali} proportion in uranium-rich areas of Athabasca bitumen nodules (Fig. 5). Similar variations were observed in the Oklo bitumen whereas the Lodève bitumen exhibits a homogeneous aliphatic-rich composition.

The proportion of aliphatic hydrocarbons in the bitumen (aliphaticity ratios, hereafter noted $\nu_{CHali}/\Sigma\nu$) has been estimated by integration of μFTIR spectra (aliphaticity ratio values calculated from all the infrared analyses are given as supplementary material). Within a given bitumen nodule of Athabasca, $\nu_{CHali}/\Sigma\nu$ define approximately concentric zonations of a few hundred micrometer radius with the presence of aliphatic-rich centers and aliphatic-poor rims (Fig. 6).

5.2. Ion microprobe $\delta^{13}C$ measurements

Carbon isotopic compositions are also strongly variable at the micrometer scale within the Athabasca bitumen with $\delta^{13}C$ values ranging from −51‰ to −23‰ (all the ion microprobe $\delta^{13}C$ values are given as supplementary material). In contrast, $\delta^{13}C$ values are rather homogeneous in Oklo and Lodève, $\delta^{13}C = -18.6 \pm 0.7$‰ (standard deviation of over 15 measurements) and -20.5 ± 1.1‰ (standard deviation of over 17 measurements), respectively. The range obtained at the micrometer scale for Athabasca bitumen is in good agreement with bulk $\delta^{13}C$ values reported for bitumen at the scale of the uranium deposits, from −53‰ to −23‰ [1–3,11]. In addition, bitumen nodules from the Athabasca show a well-defined zonation for $\delta^{13}C$ values, a zonation similar to that observed for

aliphaticity ratios, with ^{13}C-rich centers and δ^{13}C values which can range from −42‰ to −24‰ within a single nodule (Fig. 6, panel 1-a). When all the data are considered together, δ^{13}C values appear positively correlated with the aliphaticity ratios at the micrometer scale over a range from ∼−49‰ to ∼−31‰ for Athabasca bitumen (Fig. 7). It is of particular note that, in contrast, such a correlation is absent in the Oklo and Lodève bitumen.

6. Inference of organic carbon isotopics in petroleum systems

Two hypotheses will be discussed below on the possible causes for the micrometer scale variability in aliphaticity and δ^{13}C values in the bitumen nodules associated with the uranium deposits of the Athabasca. The observed concentric zonation may be due to i) reaction gradient related to bitumen precipitation/alteration processes; ii) multistage bitumen precipitation resulting from several oil events.

6.1. Carbon isotopic fractionation during bitumen precipitation and alteration

Although radiolysis has traditionally been invoked to explain the alteration of uraniferous bitumen, it cannot be the cause of the large δ^{13}C variations observed at the micrometer scale in bitumen from the Athabasca uranium deposits for two reasons. i) In fact, as thermal alteration, radiolysis reduces the content in heteroatomic and aliphatic relative to aromatic compounds [13], these changes being accompanied by an enrichment in ^{13}C [12]. Carbon isotopic fractionation is observed during artificial maturation experiments, in which the residual carbon is continuously enriched in ^{13}C as a result of the generation of ^{13}C-depleted gases. The carbon isotopic fractionation factors are at maximum between CH_4 and the organic precursors, with for instance experimentally determined values of 0.983 and 0.996 for algal and land plant kerogens, respectively [26]. Thus, the increase in δ^{13}C values observed together with a decrease of aliphatic contents during alteration stands in contrast to the trend observed in the bitumen samples from Athabasca. ii) In contrast to Athabasca bitumen nodules, the δ^{13}C values observed in the samples from Oklo (Fig. 7), which is likely radiolyzed given the high uranium content of its host-rock (42 wt.%), are rather homogeneous.

However, some radiolysis effects have been noted locally at the periphery of some of the nodules from Athabasca, within uranium-rich, discontinuous ∼50 μm wide rims, exhibiting local ^{13}C-enrichements and lower aliphaticity ratios. For instance, local ^{13}C-enrichments due to radiolysis are visible in Fig. 6 at the periphery of the bitumen nodule on the left bottom corner in panel 2-a. These effects on δ^{13}C values are however very limited, 4.6‰ at maximum. These radiolytic effects are only visible in the rim of the present bitumen nodules containing uranium inclusions (16 over 104 analyses on a total of 5 nodules). Analytical spots located in U-bearing areas exhibit low v_{CHali}, more or less $v_{C=Caro}$-enriched and $v_{C=O}$-depleted compositions relative to U-free parts of the bitumen nodules. In contrast, these compositions are similar to what can be observed in U-rich Oklo bitumen (Fig. 5). The U-bearing rims of the Athasbasca bitumen (e.g. panel 2-c in Fig. 2) are thus excluded in the following discussion.

Moreover, our results indicate that the segregation of aliphatic and non-aliphatic hydrocarbons during the precipitation of bitumen from a petroleum fluid can also be excluded as the major cause of the micrometer scale chemical and isotopic variations in the Athabasca bitumen nodules. The positive correlation between aliphaticity ratios and δ^{13}C values observed here is opposite to the systematics reported for the soluble fraction of conventional (biogenic) bitumen and petroleum: aliphatics are ^{13}C-depleted compared to aromatics ($\delta^{13}C_{aliphatics}$–$\delta^{13}C_{aromatics}$=−0.4‰ to −4‰) which are in turn ^{13}C-depleted relative to heteroatomic compounds ($\delta^{13}C_{aromatics}$–$\delta^{13}C_{heteroatomic\ compounds}$=0 to −0.79‰) [5,27–29].

6.2. Multistage bitumen precipitation resulting from several oil migration events?

Since alteration processes have been ruled out, the linear relationship between δ^{13}C values and aliphaticity ratios observed for the bitumen of Athabasca may indicate the mixing of two bitumen components, one being aliphatic-rich and having δ^{13}C values >−31‰, and the other one being aliphatic-poor and having δ^{13}C values <−49‰. However, there is no indication for the possible occurrence of source-rocks within the Athabasca Basin likely to have produced petroleum products with δ^{13}C values as low as <−49‰. As mentioned in the introduction, potential for petroleum generation has been demonstrated for several rock units in the Athabasca Basin [1,4]. Bitumen generated from Phanerozoic source-rocks and distributed in the Early Cretaceous Athabasca tar sands exhibit δ^{13}C values of ∼−30‰ [30]. Kerogen δ^{13}C values of ∼−30‰ are also reported for Mid-Proterozoic potential petroleum source-rocks identified in the Douglas Formation [1]. A genetic link with extremely low δ^{13}C bitumen (∼−49‰) is not

supported by the maximum $\delta^{13}C$ difference of ~5‰ commonly reported between kerogen and related oils (or bitumen) [25]. The lack of large C isotopic fractionation during oil generation, migration and alteration to bitumen is also supported by numerous experiments [25]. Moreover, the hypothesis that extremely low $\delta^{13}C$ bitumen may result from any petroleum source-rock to be identified across the sedimentary cover of the Athabasca Basin represents a problematic issue with regard to the general trend observed in organic carbon isotopic composition over the geological time. It has been estimated that sedimentation began in the Athabasca Basin at about 1740–1730 Ma [31], considering metamorphic ages on titanite, as young as 1750 Ma in the basement rocks [32]. Kerogens younger than 2000 Ma generally have $\delta^{13}C$ values in the −35‰ to −25‰ range, data being corrected for the effects of thermal alteration [33].

These observations raise the hypothesis of a genetic link between extremely low $\delta^{13}C$ bitumen and any extra-basinal petroleum-source rock older than 2000 Ma. In the Athabasca, carbonaceous material in the Paleoproterozoic metasedimentary rocks of the basement exhibit $\delta^{13}C$ values of −25±5‰ [3]. However, $\delta^{13}C$ values in the −40‰ to −50‰ range are commonly reported in Archean to Paleoproterozoic sedimentary rocks. For instance, $\delta^{13}C$ values as low as −45‰ have been reported for kerogen in the 3000–2300 Ma and 2700–2100 Ma source-rocks of the Witwatersrand (South Africa) and the Franceville Basins (Gabon), respectively [7,20,34]. However, timing of regional metamorphism indicates that Paleoproterozoic source-rocks may have lost their potential for hydrocarbon generation at time of bitumen emplacement (after ~1461±47 Ma [17]). The Paleoproterozoic rocks were actually metamorphosed to the amphibolite–granulite grade during the 1930 Ma Talston orogeny [6]. As a consequence, the kerogens in these rocks and the possible migrated hydrocarbon products have been metamorphosed to graphite.

This led some authors to consider an alternative origin for the solid bitumen which would have been – directly or indirectly – produced through the conversion of graphite present in basement faults to hydrocarbons during hydrothermal alteration events [3,11]. Many scenarios have been proposed in which bitumen represents (i) a solid product resulting either from graphite radiolysis or in situ hydrogenation or (ii) a precipitate resulting from the radiolytic alteration of liquid or gaseous graphite-derived hydrocarbons once migrated. However, there is no consensus on the reaction responsible for the strong carbon isotopic fractionation which could explain the large difference in $\delta^{13}C$ values observed between the extremely low $\delta^{13}C$ bitumen and graphite (−25±5‰) [3]. Thermodynamic calculations indicate that liquid hydrocarbons are generated in trace amount only by hydrothermal alteration of graphite for the P–T conditions prevailing around the Athabasca uranium deposits and geologically relevant oxygen fugacity values [35]. There are also no experimental studies supporting such hypotheses.

In the following discussion we consider the hypothesis of bitumen formation through the catalytic hydrogenation of CO_2 in the vicinity of uranium deposits. CO_2 bearing fluid was likely produced by graphite dissolution resulting from the interaction of metasedimentary basement rocks with oxidizing basinal fluids. A strong decrease in graphite content has been reported within clay-rich hydrothermal alteration haloes compared to adjacent unaltered rocks of the basement [36]. In addition, [19] observed at distances <5 km from the unconformity an intense fragmentation and deformation of graphite flakes as well as the intercalation of clay minerals in-between. Carbon isotopic study of altered graphite by [3] supports the hypothesis of graphite decomposition through oxidation to CO_2. Shear zone fluid flow pathways likely allowed the migration of CO_2-bearing fluid from the basement to the environment of the uranium deposits at the level of the unconformity.

7. Can abiogenic synthesis be responsible for the micrometer scale chemical and isotopic variations in the Athabasca bitumen?

7.1. The context of abiogenic synthesis of organic matter in the Earth's crust

Even if it has recently been demonstrated that inorganic chemical reactions make a minor contribution to hydrocarbons occurring in the Earth's crust compared to those produced by biogeochemical cycles [37], the possibility of an abiogenic origin has been previously discussed for some organic compounds in various geological environments on Earth. This includes for instance organic compounds occurring in hydrothermal ventings [38–44], in gas-emissions from volcanic areas and geothermal fields [45–47], in gas discharge from crystalline basement [37,48,49] and serpentinized ultramafic rocks [50,51], in fluid inclusions, vacuoles, grain boundaries of igneous rocks [52–55], and as films deposited on crack surfaces in crystals from mantle xenoliths [56,57]. The organic compounds in terrestrial samples for which an abiogenic origin has been discussed are mostly hydrocarbons: methane, C_2–C_5 and C_{16}–C_{19} saturated aliphatic hydrocarbons (including *n*-

alkanes, *i*-alkanes, and *neo*-alkanes), ethylene, acetylene e.g. [54,58], benzene, toluene but also include phenol and methyl phenol, benzaldehyde and benzoic acid, O-, N-heterocompounds, Cu-, Ni-organometallic compounds, chlorinated compounds [59–61], and possibly amino acids [38].

In addition, an abiogenic origin has been recently considered for some occurrences of macromolecular carbonaceous material (i.e. material insoluble in common organic solvents and containing mostly high molecular weight polymers and/or macromolecular molecules, e.g. [62]). These samples, which are also regarded by some authors as the earliest traces of life on Earth, includes graphite in apatites from the 3.8 Ga Isua supracrustal belt [63] as well as macromolecular amorphous organic matter in preserved microbe-like features or disseminated in the 3.5 Ga Apex chert of Warrawoona Group, Western Australia [64,65]. Several mechanisms are documented both experimentally and in some natural occurrences for graphite precipitation from natural carbon bearing fluids such as those containing CO_2, CO and CH_4 in geological environments [66]. In addition, thermodynamic study indicates that graphite precipitation can be achieved in the C–O–H system by several means including, for instance, the cooling of a C-bearing fluid and/or changes in ambient oxygen fugacity. In contrast to graphite, the identification of mechanisms for abiogenic macromolecular organic matter from natural systems on Earth is still elusive.

However, thermodynamic calculations by Zolotov and Shock [67] indicate that abiogenic synthesis of high molecular weight hydrocarbons is favoured under conditions prevailing during the cooling of CO, CO_2 and H_2-rich magmatic gases and at temperature ~below 250 °C through overall reactions which may be written for for *n*-alkanes and naphthalene as:

$$n\,CO + (2n+1)\,H_2 \rightarrow C_nH_{2n+2} + n\,H_2O \quad (1)$$

$$n\,CO_2 + (3n+1)\,H_2 \rightarrow C_nH_{2n+2} + 2n\,H_2O \quad (2)$$

$$10\,CO + 14\,H_2 \rightarrow C_{10}H_8 + 10\,H_2O \quad (3)$$

$$10CO_2 + 24H_2 \rightarrow C_{10}H_8 + 20H_2O \quad (4)$$

An analogy can be drawn between reactions (1) and (3) and the Fischer–Tropsch (F–T) industrial process which corresponds to the synthesis of gaseous, liquid and solid hydrocarbons, aliphatic alcohols, aldehydes, and ketones by the catalytic hydrogenation of CO using enriched synthesis gas from passage of steam over heated coke. The F–T reactions are heterogeneously catalyzed by a group VIII metal in its native form or as an oxide (e.g. Fe, Ni, Co). The initial step of the catalysis is the adsorption of gaseous CO and H_2 reactants onto the surface of the catalyst. Binding and interaction with metal atoms promotes (i) the deoxygenation of CO to give a surface carbide, (ii) the hydrogenation of surface carbide to give surface methylidyne, methylene, methyl, and eventually methane, (iii) the polymerization of adsorbed C_1 monomers to yield *n*-alkenes and *n*-alkanes and (iv) the many reactions undergone subsequently by these primary products, including hydrogenation, hydrogen migration, skeletal isomerization, cyclization, dehydrogenation, and oxidation [68].

In addition to magmatic process, a frequently inferred pathway for hydrocarbon synthesis in geological environments involves reduction of CO_2 during water–rock interaction, with minerals playing a role in generating high dissolved H_2 concentrations [69]. Fe-bearing minerals (e.g. magnetite and montmorillonite) as well as Fe–Ni alloys have been shown to provide catalytic surfaces during hydrogenation of CO_2 [70,71]. It has been proposed that the abiogenic reduction of inorganic carbon to hydrocarbons could be favoured by the serpentinization reactions occurring in hydrothermally altered ultramafic rocks [72]. Shock [73] showed from theoretical considerations that the hydrogenation of aqueous CO_2 to organic compounds is favourable in the oceanic crust under hydrothermal conditions (temperature below 500 °C). However, the potential for formation of hydrocarbons other than CH_4 during serpentinization reactions remains to be demonstrated experimentally [69,72]. More recently, [74] experiments demonstrated the potential of alternative geological processes such as the thermal decomposition of siderite at 350 °C in presence of water to form abiogenic high molecular weight hydrocarbons and macromolecular organic matter [74]. These authors indicate that synthesis of organic compounds other than CH_4 may proceed in these experiments from reduction of CO_2 in water-saturated vapour phase. All these results support the view that an abiogenic origin is worth to be discussed for solid organic matter in some local environments of the Earth's crust, in the absence of biological indicators such as biomarkers or microfossils.

Chemical and physical conditions prevailing during the formation of uranium deposits of the Athabasca Basin (Saskatchewan, Canada) may offer favourable conditions for abiogenic synthesis of hydrocarbons through catalytic hydrogenation of CO_2 for 3 main reasons. (i) Some studies report [71,75] the production of lipids (including oxygenated and hydrocarbon compounds with carbon numbers up to 40) during

experimental hydrogenation of CO_2 in the temperature window of 150–400 °C with a maximum yield at ~200 °C. These temperature conditions are close to those derived from fluid inclusions studies to have prevailed during the formation of the deposits (180 °C, 600 bar) [10]; (ii) Hematite, which may constitute a catalyst of hydrogenation reactions is abundant in the vicinity of the ores [6]; (iii) The reactants of the hydrocarbon synthesis through catalytic hydrogenation processes such as reactions (2) and (4) are also available in the environment of uranium deposits. The presence of H_2 and CO_2 has been demonstrated in the gas-phase of fluid inclusions in both the basement and the altered sandstone cover, H_2 being interpreted as the product of water radiolysis [10,76].

7.2. An abiogenic origin for the chemical and $\delta^{13}C$ variability of the Athabasca bitumen?

It appears that the fractionation related to the catalytic conversion of CO_2 to hydrocarbons may explain both (i) the carbon isotopic compositions and (ii) their variation as a function of the aliphaticity ratios in bitumen in the Athabasca uranium deposits.

The bulk $\delta^{13}C$ values reported for the bitumen of Athabasca ranging from −53‰ to −23‰ [1–3,11] are consistent with values expected for the catalytic conversion of CO_2 to hydrocarbons. Several studies of the catalytic hydrogenation of CO to high molecular weight (HMW) hydrocarbons under dry H_2 atmosphere showed variable kinetic carbon isotopic fractionations ($\alpha_{HMW\ hydrocarbons–CO}$), ranging from 0.965 to 0.990 [77–80] for a review. In addition, a recent study of hydrocarbon synthesis during the decomposition of siderite under hydrothermal conditions indicates a carbon isotope fractionation of ~0.964 between C_{10}–C_{26} hydrocarbons and dissolved CO_2 ($\alpha_{C10–C26\ hydrocarbons–CO_2}$) [81]. Similar isotopic fractionations have been obtained during experimental hydrogenation of dissolved CO_2 to CH_4, with $\alpha_{CH_4–CO2}$ ranging from 0.940 to 0.965 [70]. Carbon isotopic composition of the CO_2-bearing fluids has not been measured, but it is highly probable that CO_2 has been produced by the decomposition of basement graphite during the percolation of the oxidizing basinal fluids [3]. Assuming a temperature of 180°C for the percolating fluids [10], a $\delta^{13}C$ value close to −10±5‰ can be calculated at isotopic equilibrium for CO_2-bearing fluids, taking $\delta^{13}C=-25\pm5$‰ for the graphite (as measured in [3]). This calculated value is in good agreement with the $\delta^{13}C$ value of −7‰ measured in calcite paragenetically associated with bitumen ($\alpha_{calcite–CO_2}=1.004$) [10]. As a first approximation, a carbon isotopic effect analogous to that related to the abiogenic formation of HMW hydrocarbons from CO ($\alpha_{HMW\ hydrocarbons–CO}$) has been considered between reacting CO_2 and the synthesized bitumen. The $\delta^{13}C$ values which can be predicted for the bulk hydrocarbons produced (from −45±5‰ to −20±5‰) overlap the $\delta^{13}C$ range observed for bulk bitumen from Athabasca (from −53‰ to −23‰).

In contrast to biogenic hydrocarbons, a positive difference in $\delta^{13}C$ between saturated and unsaturated hydrocarbons is systematically produced in gas synthesized through dynamic FT synthesis reactions [78,79]. This is also observed for abiogenic volatile hydrocarbons produced by spark discharge in methane [82] and for hydrocarbons extracted from synthetic oils produced by thermocatalysis of oleic acid [83]. It should be noted that no isotopic results are available yet for alkenes and alcohols produced together with *n*-alkanes in synthesis experiment from dissolved CO_2 by [81]. The differences in $\delta^{13}C$ between saturated and unsaturated hydrocarbons reported in the literature range

Table 1
Carbon isotopic fractionation between saturated and unsaturated hydrocarbons during abiogenic synthesis experiments

Synthesis experiments	Hydrocarbons products analyzed		$\delta^{13}C_{saturated}–\delta^{13}C_{unsaturated}$
	Saturated	Unsaturated	(‰)
Spark discharge in CH_4 [a]	C_2H_6	C_2H_4	+3.7±0.3
		C_2H_2	+4.9±0.3
Thermocatalysis of oleic acid [b]	*n*-alkanes	PAHs [c]	+2
Open-flow FT processes involving CO and H_2 [d]	*n*-C_2–C_5 alkanes	C_3H_6	+7
Open-flow FT processes involving CO and H_2 [e]	LMWHCs [f]	LMWHCs [f]	+3–19

[a] [82].
[b] [83].
[c] Polynuclear aromatic hydrocarbons.
[d] [78].
[e] [79].
[f] Low molecular weight hydrocarbons.

from +2 to +19‰ (Table 1). Thus, the mixing in various proportions of aliphatic and aromatic hydrocarbons produced through abiogenic reactions may explain the positive correlation observed between the aliphaticity ratios and carbon isotopic compositions in the bitumen of the Athabasca uranium deposits (Fig. 7). This may also explain the observed $\delta^{13}C$ difference between aliphatics and non-aliphatics of at least +18‰ for the Athabasca bitumen, although this value is in the extreme range of available experimental data.

According to this hypothesis, the chemical zonation observed in Athabasca bitumen nodules may reflect a decreasing H_2 content of the gas phase through time. This would have resulted in a decreasing production of aliphatics vs. non-aliphatic [84] hydrocarbons during the growth of the nodules from the center to the edge. This hypothesis is in good agreement with the lack of large $\delta^{13}C$ variability at the micrometer scale associated with a ^{13}C-enrichment of aliphatics relative to non-aliphatics in the bitumen of demonstrated biogenic origin from Oklo and Lodève uranium deposits [7,9]. In contrast, a parallel can be drawn between our results and the observation that isotopic zoning and small isotopic shifts at the millimeter-scale are common features in fluid-deposited graphite, by contrast with graphite resulting from the metamorphic conversion of sedimentary organic matter [66].

8. Conclusion

In regard to the geological setting as well as the unusual relationship between aliphaticity and $\delta^{13}C$ values of the bitumen samples from the Athabasca uranium deposits, an abiogenic origin can be considered as a reasonable hypothesis for the bitumen of the Athabasca. This may also explain the extremely low $\delta^{13}C$ values of some of this bitumen. Obviously, the amount of abiogenic organic matter found in the Athabasca uranium deposits is minor compared to the layered bitumen commonly observed in uranium deposits associated to conventional petroleum deposits (e.g. Oklo and Lodève). However, the present results are in agreement with the growing recognition that, contrary to the general view, ^{13}C-depleted carbon isotopic composition in organic matter cannot be considered as an unequivocal evidence for a biogenic origin [80,81,85–87]. A criterion for abiogenic origin of low molecular weight alkanes has been recently proposed from the positive correlation between $\delta^{13}C$ values and the carbon number observed for C_1–C_4 gases recovered from boreholes in the Canadian Shield [37]. The bitumen from the Athabasca uranium deposits shows at the micrometer scale a similar relationship with a correlated increase in $\delta^{13}C$ and aliphaticity (Fig. 7). The present results suggest that this relationship may be used as a criterion for "abiogenicity" and may be applied in future studies to organic matter in Early Archean or extraterrestrial samples investigated for traces of life.

Acknowledgements

This research was carried out thanks to a Ph.D. grant from the French Research Ministry. We thank M. Champenois, E. Deloule, D. Mangin and C. Rollion-Bard for assistance with ion microprobe analyses, C. France-Lanord and C. Guillemette for help in gas source mass spectrometry, A. Izart for providing standards, O. Barrès and P. De Donato for facilities for μFTIR analyses, L. Richard and M. Roskosz for discussions and throughout correction of the manuscript. COGEMA Resources Inc. (Areva) is also acknowledged for provision of some samples.

Appendix A. Supplementary data

Supplementary data associated with this article can be found, in the online version, at doi:10.1016/j.epsl.2007.03.018.

References

[1] P. Landais, J.M. Dereppe, A chemical study of the carbonaceous material from the Carswell structure, Geological Association of Canada special paper — The Carswell Structure Uranium Deposits, Saskatchewan, vol. 29, Geological Survey of Canada, Toronto, 1985, pp. 165–174.
[2] J.S. Leventhal, R.I. Grauch, C.N. Threlkeld, F.E. Lichte, Unusual organic matter associated with uranium from the Claude deposit, Cluff Lake, Canada, Econ. Geol. 82 (1987) 1169–1176.
[3] T.K. Kyser, M.R. Wilson, G. Ruhrmann, Stable isotope constraints on the role of graphite in the genesis of unconformity-type uranium deposits, Can. J. Earth Sci. 26 (1989) 490–498.
[4] N.S.F. Wilson, L.D. Stasiuk, M.G. Fowler, Post-mineralization origin of organic matter in Athabasca unconformity uranium deposits, Saskatchewan, Canada, Summary of investigations 2002, Saskatchewan Geological Survey, vol. 2, 2002, 6p.
[5] J.A. Curiale, Origin of solid bitumens, with emphasis on biological marker result, Org. Geochem. 10 (1986) 559–580.
[6] V. Ruzicka, Unconformity-associated uranium, in: O.R. Eckstrand, W.D. Sinclair, R.I. Thorpe (Eds.), Geology of Canadian Mineral Deposit Types, vol. 8, Geological Survey of Canada, Toronto, 1996, pp. 197–210.
[7] F. Gauthier-Lafaye, F. Weber, The Francevillian (Lower Proterozoic) uranium ore deposits of Gabon, Econ. Geol. 84 (1989) 2267–2285.
[8] B. Nagy, F. Gauthier-Lafaye, P. Holliger, D.W. Davis, D.J. Mosmann, J.S. Leventahl, M.J. Rigali, J. Parnell, Role of organic

matter in containment of uranium and fissiongenic isotopes at the Oklo natural reactor, Nature 354 (1991) 472–475.
[9] P. Landais, Organic geochemistry of sedimentary uranium ore deposits, Ore Geol. Rev. 11 (1996) 33–51.
[10] D. Derome, Evolution et origines des saumures dans les bassins protérozoïques au voisinage de la discordance socle/couverture. L'exemple de l'environnement des gisements d'uranium associés aux bassins Kombolgie (Australie) et Athabasca (Canada), Ph.D. thesis, Université Henri Poincaré, France, 2002.
[11] P. Landais, J. Dubessy, J.M. Dereppe, R.P. Philp, Characterization of graphite alteration and bitumen genesis in the Cigar Lake deposit (Saskatchewan, Canada), Can. J. Earth Sci. 30 (1993) 743–753.
[12] J.S. Leventhal, C.N. Threlkeld, Carbon-13/Carbon-12 isotope fractionation of organic matter associated with uranium ores induced by alpha irradiation, Science 202 (1978) 430–432.
[13] P.A. Eakin, Isotopic and petrographic studies of uraniferous hydrocarbons from around the Irish Sea Basin, J. Geol. Soc. (Lond.) 146 (1989) 663–673.
[14] O. Ruau, B. Pradier, P. Landais, J.L. Gardette, Influence of the conditions of deposition on the chemistry and the reflectance variations of the Brent coals, Org. Geochem. 25 (1996) 325–339.
[15] L. Sangély, M. Chaussidon, R. Michels, V. Huault, Microanalysis of carbon isotopic composition in organic matter by secondary ion mass spectrometry, Chem. Geol. 223 (2005) 179–195.
[16] J. Hoeve, T.I.I. Sibbald, On the genesis of Rabbit Lake and the other unconformity-type uranium deposits in Northern Saskatchewan, Canada, Econ. Geol. 73 (1978) 1450–1473.
[17] M. Fayek, T.M. Harrison, R.C. Ewing, M. Grove, C.D. Coath, O and Pb isotopic analyses of uranium minerals by ion microprobe and U–Pb ages from the Cigar Lake deposit, Chem. Geol. 185 (2002) 205–225.
[18] G. Lorilleux, M. Jebrak, M. Cuney, D. Baudemont, Polyphase hydrothermal breccias associated with unconformity-related uranium mineralization (Canada): from fractal analysis to structural significance, J. Struct. Geol. 24 (2002) 323–338.
[19] A. Wang, P. Dhamelincourt, J. Dubessy, D. Guérard, P. Landais, M. Lelaurain, Characterization of graphite alteration in an uranium deposit by micro-Raman spectroscopy, X-ray diffraction, transmission electron microscopy and scanning electron microscopy, Carbon 27 (1989) 209–218.
[20] D.J. Mossman, F. Gauthier-Lafaye, S.E. Jackson, Carbonaceous substances associated with the Paleoproterozoic natural nuclear fission reactors of Oklo, Gabon: paragenesis, thermal maturation and carbon isotopic and trace element compositions, Precambrian Res. 106 (2001) 135–148.
[21] J.R. Lancelot, B. de Saint André, H. de la Boisse, Systématique U–Pb et évolution du gisement d'uranium de Lodève, Miner. Depos. 19 (1984) 44–53.
[22] P.G. Rouxhet, P.L. Robin, G. Nicaise, Characterization of kerogens and of their evolution by infrared spectroscopy, in: B. Durand (Ed.), Kerogen, Editions Technip, Paris, 1980, pp. 163–190.
[23] P. Landais, A. Rochdi, In situ examination of coal macerals oxidation by micro-FT-i.r. spectroscopy, Fuel 72 (1993) 1393–1401.
[24] S.H. Wang, P.R. Griffiths, Resolution enhancement of diffuse reflectance IR spectra of coals by Fourier self deconvolution I: C–H stretching and bending modes, Fuel 64 (1985) 229–236.
[25] L. Sangély, Development of in situ isotopic analysis in organic carbon by ion microprobe: contribution to the study of the origin of bitumen associated with uranium deposits of the Athabasca (Canada) and the Witwatersrand (South Africa), Ph.D. thesis, Institut National Polytechnique de Lorraine, France, 2004.
[26] U. Berner, E. Faber, G. Scheeder, D. Panten, Primary cracking of algal and landplant kerogens: kinetic models of isotope variations in methane, ethane and propane, Chem. Geol. 126 (1995) 233–245.
[27] W.J. Stahl, Source rock–crude oil correlation by isotopic type-curves, Geochim. Cosmochim. Acta 42 (1978) 1573–1577.
[28] Z. Sofer, Stable isotope compositions of crude oils: application to source depositional environments and petroleum alteration, Am. Assoc. Pet. Geol. Bull. 68 (1984) 31–49.
[29] V.E. Andrusevich, M.H. Engel, J.E. Zumberge, L.A. Brothers, Secular, episodic changes in stable carbon isotope composition of crude oils, Chem. Geol. 152 (1998) 59–72.
[30] K.N. Jha, J. Gray, O.P. Strausz, The isotopic composition of carbon in the Alberta oil sand, Geochim. Cosmochim. Acta 43 (1979) 1571–1573.
[31] R.H. Rainbird, R.A. Stern, N. Rayner, C.W. Jefferson, Age, provenance, and regional correlation of the Athabasca Group, Saskatchewan and Alberta, constrained by igneous and detrital zircon geochronology, in: C.W. Jefferson, G. Delaney (Eds.), EXTECH IV: Geology and Uranium EXploration TECHnology of the Proterozoic Athabasca Basin, Saskatchewan and Alberta, Geological Survey of Canada, 2005.
[32] S.E. Orrell, M.E. Bickford, J.F. Lewry, Crustal evolution and age of thermometric reworking in the Western hinterland of the Trans-Hudsonian orogen, Northern Saskatchewan, Precambrian Res. 95 (1999) 187–223.
[33] D.J. Des Marais, Isotopic evolution of the biogeochemical carbon cycle during the Proterozoic Eon, Org. Geochem. 27 (1997) 185–193.
[34] Y. Watanabe, H. Naraoka, D.J. Wronkiewicz, K.C. Condie, H. Ohmoto, Carbon, nitrogen, and sulfur geochemistry of Archean and Proterozoic shales from the Kaapvaal Craton, South Africa, Geochim. Cosmochim. Acta 61 (1997) 3441–3459.
[35] L. Richard, L. Sangély, Thermodynamic and carbon isotopic constraints on the origin of unusual bitumens in the uranium deposits of Athabasca (Saskatchewan, Canada), 14th Annual Goldschmidt Conference, Copenhagen, Denmark, 2004.
[36] P. Bruneton, Geology of the Cigar Lake uranium ore-deposit (Saskatchewan, Canada), in: C.F. Gilboy, L.W. Viagrass (Eds.), Economic Minerals of Canada, vol. 8, Saskatchewan Geological Special Publication, Toronto, 1987, pp. 99–119.
[37] B. Sherwood-Lollar, T.D. Westgate, J.A. Ward, G.F. Slater, G. Lacrampe-Couloume, Abiogenic formation of alkanes in the Earth's crust as a minor source for global hydrocarbon reservoirs, Nature 416 (2002) 522–524.
[38] D.E. Ingmanson, M.J. Dowler, Unique amino acid composition of Red Sea brine, Nature 286 (1980) 51–52.
[39] J.A. Welhan, H. Craig, Methane, hydrogen and helium in hydrothermal fluids at 21 degrees N on the East Pacific Rise, in: P.A. Rona, K. Bostroem, L. Laubier, K.L. Smith Jr. (Eds.), Hydrothermal Processes at Seafloor Spreading Centers, Plenum Press, New York, USA, 1983, pp. 391–409.
[40] J.A. Welhan, J.E. Lupton, Light hydrocarbon gases in Guaymas Basin hydrothermal fluids: thermogenic versus abiogenic origin, Am. Assoc. Petrol. Geol. Bull. 71 (1987) 215–223.
[41] R. Botz, D. Stüben, G. Winckler, R. Bayer, M. Schmitt, E. Faber, Hydrothermal gases offshore Milos Island, Greece, Chem. Geol. 130 (1996) 161–173.
[42] N.G. Holm, J.L. Charlou, Initial indications of abiotic formation of hydrocarbons in the Rainbow ultramafic hydrothermal system, Mid-Atlantic Ridge, Earth Planet. Sci. Lett. 191 (2001) 1–8.

[43] C. Riedel, M. Schmidt, R. Botz, F. Theilen, The Grimsey hydrothermal field offshore North Iceland: crustal structure, faulting and related gas venting, Earth Planet. Sci. Lett. 193 (2001) 409–421.
[44] J.L. Charlou, J.P. Donval, Y. Fouquet, B.P. Jean, N. Holm, Geochemistry of high H_2 and CH_4 vent fluids issuing from ultramafic rocks at the Rainbow hydrothermal field (36 degrees 14N, MAR), Chem. Geol. 191 (2002) 345–359.
[45] T.M. Gerlach, Chemical characteristics of the volcanic gases from Nyiragongo lava lake and the generation of CH_4-rich fluid inclusions in alkaline rocks, J. Volcanol. Geotherm. Res. 8 (1980) 177–189.
[46] N.E. Podkletnov, E.K. Markhinin, New data on abiogenic synthesis of prebiological compounds in volcanic processes, Orig. Life Evol. Biosph. 11 (1981) 303–315.
[47] B. Capaccioni, M. Martini, F. Mangani, L. Giannini, G. Nappi, F. Prati, Light hydrocarbons in gas-emissions from volcanic areas and geothermal fields, Geochem. J. 27 (1993) 7.
[48] B. Sherwood-Lollar, S.K. Frape, S.M. Weise, P. Fritz, S.A. Macko, J.A. Welhan, Abiogenic methanogenesis in crystalline rocks, Geochim. Cosmochim. Acta 57 (1993) 5087–5097.
[49] B. Sherwood Lollar, G. Lacrampe-Couloume, G.F. Slater, J. Ward, D.P. Moser, T.M. Gihring, L.-H. Lin, T.C. Onstott, Unravelling abiogenic and biogenic sources of methane in the Earth's deep subsurface, Chem. Geol. 226 (2006) 328–339.
[50] T.A. Abrajano, N.C. Sturchio, J.K. Bohlke, G.L. Lyon, R.J. Poreda, C.M. Stevens, Methane-hydrogen gas seeps, Zambales Ophiolite, Philippines: deep or shallow origin? Chem. Geol. 71 (1988) 211–222.
[51] T.A. Abrajano, N.C. Sturchio, B.M. Kennedy, G.L. Lyon, K. Muehlenbachs, J.K. Bohlke, Geochemistry of reduced gas related to serpentinization of the Zambales ophiolite, Philippines, Appl. Geochem. 5 (1990) 625–630.
[52] I.A. Petersilie, H. Sörensen, Hydrocarbon gases and bituminous substances in rocks from the Ilimaussaq alkaline intrusion, South Greenland, Lithos 3 (1970) 59–76.
[53] D.S. Kelley, Methane-rich fluids in the oceanic crust, J. Geophys. Res. 101 (B2) (1996) 2943–2962.
[54] S. Salvi, A.E. Williams-Jones, Fischer-tropsch synthesis of hydrocarbons during sub-solidus alteration of the Strange Lake peralkaline granite, Quebec/Labrador, Canada, Geochim. Cosmochim. Acta 61 (1997) 83–99.
[55] D. Kelley, G. Früh-Green, Abiogenic methane in deep-seated mid-ocean ridge environments: insights from stable isotope analyses, J. Geophys. Res. 104 (B5) (1999) 10,439–10,460.
[56] E.A. Mathez, Carbonaceous matter in mantle xenoliths: composition and relevance to the isotopes, Geochim. Cosmochim. Acta 51 (1987) 2339–2347.
[57] R. Sugisaki, K. Mimura, Mantle hydrocarbons: abiotic or biotic? Geochim. Cosmochim. Acta 58 (1994) 2527–2542.
[58] N.G. Holm, J.L. Charlou, Initial indications of abiotic formation of hydrocarbons in the Rainbow ultramafic hydrothermal system, Mid-Atlantic Ridge, Earth Planet. Sci. Lett. 191 (2001) 1–8.
[59] T.N. Tingle, M.F. Hochella Jr., C.H. Becker, R. Malhotra, Organic compounds on crack surfaces in olivine from San Carlos, Arizona and Hualalai Volcano, Hawaii, Geochim. Cosmochim. Acta 54 (1990) 477–485.
[60] T.N. Tingle, E.A. Mathez, M.F. Hochella Jr., Carbonaceous matter in peridotites and basalts studied by XPS, SALI, and LEED, Geochim. Cosmochim. Acta 55 (1991) 1345–1352.
[61] E.A. Mathez, D.M. Mogk, Characterization of carbon compounds on a pyroxene surface from a gabbro xenolith in basalt by time-of-flight secondary ion mass spectrometry, Am. Mineral. 83 (1998) 918–924.
[62] M.A. Sephton, I. Gilmour, Pyrolysis-gas chromatography-isotope ratio mass spectrometry of macromolecular material in meteorites, Planet. Space Sci. 49 (2001) 465–471.
[63] M.A. Van Zuilen, A. Lepland, G. Arrhenius, Reassessing the evidence for the earliest traces of life, Nature 418 (2002) 627–630.
[64] M.D. Brasier, N.V. Grassineau, O.R. Green, A.P. Jephcoat, A.K. Kleppe, M.J. Van Kramendonk, J.F. Lindsay, A. Steele, Questioning the evidence of Earth's oldest fossils, Nature 416 (2002) 76–81.
[65] J.D. Pasteris, B. Wopenka, Necessary but not sufficient: Raman identification of disordered carbon as a signature of ancient life, Astrobiology 3 (2003) 727–738.
[66] F.J. Luque, J.D. Pasteris, B. Wopenka, M. Rodas, J.F. Barrenenechea, Natural fluid-deposited graphite: mineralogical characteristics and mechanisms of formation, Am. J. Sci. 298 (1998) 471–498.
[67] M.Y. Zolotov, E.L. Shock, A thermodynamic assessment of the potential synthesis of condensed hydrocarbons during cooling and dilution of volcanic gases, J. Geophys. Res. 105 (B1) (2000) 539–559.
[68] P.M. Maitlis, Fischer–Tropsch, organometallics, and other friends, J. Organomet. Chem. 689 (2004) 4366–4374.
[69] T.M. McCollom, J.S. Seewald, A reassessment of the potential reduction of dissolved CO_2 to hydrocarbons, Geochim. Cosmochim. Acta 65 (2001) 3769–3778.
[70] J. Horita, M.E. Berndt, Abiogenic methane formation and isotopic fractionation under hydrothermal conditions, Science 285 (1999) 1055–1057.
[71] T.M. McCollom, G. Ritter, B.R.T. Simoneit, Lipd synthesis under hydrothermal conditions by Fischer–Tropsch-type reactions, Orig. Life Evol. Biosph. 29 (1999) 153–166.
[72] M.E. Berndt, D.E. Allen, W.E.J. Seyfried, Reduction of CO_2 during serpentinization of olivine at 300 °C and 500 bar, Geology 24 (1996) 351–354.
[73] E.L. Shock, Geochemical constraints on the origin of organic compounds in hydrothermal systems, Orig. Life Evol. Biosph. 20 (1990) 331–367.
[74] T.M. McCollom, Formation of meteorite hydrocarbons from thermal decomposition of siderite ($FeCO_3$), Geochim. Cosmochim. Acta 67 (2003) 311–317.
[75] A.I. Rushdi, B.R.T. Simoneit, Lipid formation by aqueous Fischer–Tropsch-type synthesis over a temperature range of 100 to 400 °C, Orig. Life Evol. Biosph. 31 (2001) 103–118.
[76] J. Dubessy, M. Pagel, J.M. Beny, H. Christensen, B. Hickel, C. Kosztolany, B. Poty, Radiolysis evidenced by H_2–O_2 and H_2 bearing fluid inclusions in three uranium deposits, Geochim. Cosmochim. Acta 52 (1988) 1155–1167.
[77] M.S. Lancet, E. Anders, Carbon isotope fractionation in the Fischer–Tropsch synthesis and in meteorites, Science 170 (1970) 980–982.
[78] K. Wedeking, R. Ship, S. Chang, E. Rightor, T.J. Pinnavaia, Carbon isotopic compositions of individual hydrocarbons, carbon dioxide, and oils from the Fischer–Tropsch reaction, 16th Lunar and Planetary Science Conference, Houston, USA, 1985.
[79] G.U. Yuen, J.A. Pecore, J.F. Kerridge, T.J. Pinnavaia, E.G. Rightor, Carbon isotopic fractionation in Fischer–Tropsch type reactions, 21st Lunar and Planetary Science Conference, Houston, USA, 1990.
[80] J. Horita, Some perspectives on isotope biosignatures for early life, Chem. Geol. 218 (2005) 171–186.

[81] T.M. McCollom, J.S. Seewald, Carbon isotope composition of organic compounds produced by abiotic synthesis under hydrothermal conditions, Earth Planet. Sci. Lett. 243 (2006) 74–84.
[82] S. Chang, D. Des Marais, R. Mack, S.L. Miller, G.E. Strathearn, Prebiotic organic syntheses and the origin of life, in: W.J. Schopf (Ed.), Earth's Earliest Biosphere — Its Origin and Evolution, Princeton Univ. Press, Princeton, 1983, pp. 53–92.
[83] E.M. Galimov, The Biological Fractionation of Isotopes, Academic Press Inc, Orlandor, 1985.
[84] G.P. van der Laan, Kinetics, selectivity and scale up of the Fischer–Tropsch synthesis, Ph. D. thesis, Groningen University, Netherlands, 1999.
[85] P. Szatmari, Petroleum formation by Fischer–Tropsch synthesis in plate tectonics, Am. Assoc. Pet. Geol. Bull. 73 (1989) 989–998.
[86] E.M. Galimov, Isotopic criteria for identification of organic carbon on Earth and meteorites, Space Sci. Rev. 106 (2003) 249–262.
[87] M. Brasier, O. Green, J. Lindsay, A. Steele, Earth's oldest (3.5 Ga) fossils and the "early eden hypothesis": questioning the evidence, Orig. Life Evol. Biosph. 34 (2004) 257–269.